

Matching perturbative and Parton Shower corrections to Bhabha process at flavour factories

Giovanni Balossini^a Carlo M. Carloni Calame^{b,a,*}
 Guido Montagna^{a,b} Oreste Nicosini^{b,a} Fulvio Piccinini^{b,a}

^a*Dipartimento di Fisica Nucleare e Teorica, Università di Pavia
 Via A. Bassi 6, 27100, Pavia, Italy*

^b*Istituto Nazionale di Fisica Nucleare, sezione di Pavia
 Via A. Bassi 6, 27100, Pavia, Italy*

Abstract

We report on a high-precision calculation of the Bhabha process in Quantum Electrodynamics, of interest for precise luminosity determination of electron-positron colliders involved in R measurements in the region of hadronic resonances. The calculation is based on the matching of exact next-to-leading order corrections with a Parton Shower algorithm. The accuracy of the approach is demonstrated in comparison with existing independent calculations and through a detailed analysis of the main components of theoretical uncertainty, including two-loop corrections, hadronic vacuum polarization and light pair contributions. The calculation is implemented in an improved version of the event generator BABAYAGA with a theoretical accuracy of the order of 0.1%. The generator is now available for high-precision simulations of the Bhabha process at flavour factories.

Key words: Quantum Electrodynamics; Bhabha process; luminosity; next-to-leading order corrections; two-loop corrections; Parton Shower
PACS: 12.15.Lk, 12.20.-m, 13.40.Ks, 13.66.Jn

1 Introduction

The determination of the R ratio in electron-positron annihilation, defined as $R = \sigma(e^+e^- \rightarrow \text{hadrons})/\sigma(e^+e^- \rightarrow \mu^+\mu^-)$, is a classical measurement of

* Corresponding author. E-mail address: carlo.carloni.calame@pv.infn.it

particle physics and still a quantity of deep interest in modern research about the fundamental constituents of matter. The measurement of the cross section for electron-positron annihilation into hadrons is, in fact, an important task of high-luminosity colliders operating in the region of hadronic resonances, such as Φ , τ -charm and B factories [1]. The reason is that the R value is crucial for precise predictions of the hadronic contribution to $(g-2)_\mu$, the anomalous magnetic moment of the muon [2], and to the running of the electromagnetic coupling from its value at low energy up to high energies [3]. In particular, the QED coupling constant evaluated at Z pole $\alpha_{QED}(M_Z)$ is a fundamental ingredient in precision tests of the electroweak theory and its uncertainty critically limits the bound on the Higgs boson mass in the indirect search through fits to precision data [4].

The R value has been measured by many experiments from hadron production threshold to the mass of the Z boson. Below the bottom threshold and, especially, in the energy range below 5 GeV, precision measurements of R are motivated by reducing the uncertainty of the hadronic contribution to $(g-2)_\mu$ and $\alpha_{QED}(M_Z)$. The experimental methods presently employed to determine R include direct measurements and indirect measurements of the hadron production cross section [5]. The first approach is followed in the recent measurements by CMD-2 and SND collaborations at VEPP-2M [6], BES at BEPC [7] and CLEO at CESR [8]. The indirect measurement, which makes use of the emission of one or more hard photons from the initial state and is known as radiative return [9], is presently performed by KLOE collaboration at DAΦNE [10] and BABAR at PEP-II [11], and is under consideration by BELLE at KEK-B. The radiative return is of particular interest because it enables, in principle, to measure R over the full energy range, i.e. from hadron production threshold to the nominal centre-of-mass energy.

Independently from the different types of error affecting the precision of the two methods, a common source of systematic uncertainty comes from the knowledge of the collider luminosity. To keep under control such an uncertainty, high-precision calculations of the QED processes $e^+e^- \rightarrow e^+e^-$, $\mu^+\mu^-$, $\gamma\gamma$, and relative Monte Carlo generators, are required. Among the QED processes, the large-angle Bhabha scattering is of particular interest because of its large cross section and its clean experimental signature. To simulate the experimentally relevant distributions and calculate the cross section of the Bhabha process, KLOE and CLEO collaborations make use of the QED Parton Shower generator BABAYAGA, developed in Refs. [12,13] with a precision target of 0.5%. The Monte Carlo MCGPJ [14], which includes exact $\mathcal{O}(\alpha)$ corrections supplemented with leading logarithmic higher-order contributions and has an estimated accuracy of about 0.2%, is presently used at VEPP-2M to monitor the collider luminosity. To keep under control the theoretical precision, other codes, such as the $\mathcal{O}(\alpha)$ generator of Ref. [15] (based on Ref. [16]) and the Yennie-Frautschi-Suura tool BHWIDE [17], are also employed by the

experimental collaborations. A generally good agreement between theory and data, as well as between the results of the different generators, is observed, thus confirming the precision claims of the respective calculations [10,14,18].

Nevertheless, further progress in the calculation of radiative corrections to QED processes and, in particular, the development of precise large-angle Bhabha generators are still required. This is motivated by a number of reasons. First, the total luminosity error quoted by KLOE is presently 0.6% [10], where the dominant source of uncertainty comes from theory, i.e. from the 0.5% physical precision inherent the **BABAYAGA** generator. The reduction of such an error demands progress on the Bhabha theory side. Secondly, the measurement of the hadronic cross section in the $\pi^+\pi^-$ channel at VEPP-2M has achieved a total systematic error of 0.6–1% in the region of the ρ resonance [6], which requires, in turn, an assessment of the collider luminosity at the level of 0.1%. Last but not least, precision measurements of R through radiative return at high-luminosity e^+e^- storage rings KEK-B and PEP-II are already performed or foreseen in the near future, as previously mentioned. These facts are also among the motivations of the recent efforts in the direction of complete two-loop calculations to Bhabha scattering [19,20,21,22,23,24]. The need for keeping under control accurately radiative corrections to QED processes has been recently reinforced by the update of the $e^+e^- \rightarrow \pi^+\pi^-$ cross section by SND collaboration at VEPP-2M. This reanalysis [25], which leads to a decrease of the measured cross section by two systematic errors in average with respect to the previous one, became necessary due to a flaw in the Monte Carlo generators previously used in data analysis to compute radiative corrections to $e^+e^- \rightarrow \pi^+\pi^-$ and $e^+e^- \rightarrow \mu^+\mu^-$.

The aim of the present paper is to report on a high-precision calculation of radiative corrections to the Bhabha process, in order to improve the theoretical formulation of the original **BABAYAGA** generator down to $\mathcal{O}(0.1\%)$. The approach is based on the matching of exact next-to-leading-order corrections with resummation through all orders of α of the leading contributions from multiple soft and collinear radiation, which are taken into account according to a QED Parton Shower.¹ Emphasis is also put on the impact of higher-order non-leading-log corrections, such as $\alpha^2 L$ (with L collinear logarithm), and non-photonic light pair contributions, to arrive at a sound estimate of the overall theoretical error. A critical comparison of the formulation presented in

¹ It is worth stressing that the matching procedure here developed allows for a fully exclusive generation of multiple-photon radiation. With respect to different exclusive exponentiation approaches, such as the Yennie-Frautschi-Suura method [26], the present approach differs in some implementation details and, in particular, in the resummation of non-infrared single collinear logarithms. However, since both formalisms coincide at first order, the differences start at $\mathcal{O}(\alpha^2)$ and are not infrared sensitive.

this paper with existing two-loop calculations allows to put on a more quantitative ground the estimated theoretical uncertainty.

The paper is organized as follows. In Sect. 2 we describe in detail the matching of next-to-leading-order corrections with Parton Shower, which the old version of **BABAYAGA** was based on. In Sect. 3 the predictions for large-angle Bhabha scattering of the improved version of **BABAYAGA** are compared with those of independent generators, both for integrated cross sections and differential distributions of experimental interest. In Sect. 4 different sources of theoretical uncertainties are investigated: vacuum polarization uncertainty, approximate treatment of two real photon emission, light pair corrections, missing virtual plus soft corrections to one real photon emission. Section 4.4 is devoted to the comparison of the formulation implemented in **BABAYAGA**, expanded at $\mathcal{O}(\alpha^2)$, with two existing calculations of next-to-next-to-leading-order corrections to Bhabha scattering: the purely photonic contribution (virtual plus soft-real corrections) and the two-loop $N_f = 1$ complete calculation in the soft-pair approximation for real pair production. These comparisons corroborate the claimed physical precision of **BABAYAGA** of $\mathcal{O}(0.1\%)$. It is worth stressing that, even with a complete two-loop calculation at hand, the effect of higher order corrections is still relevant on the scale of 0.1% accuracy, as proved in Sect. 4.1. Conclusions and possible developments are given in Sect. 5.

2 Matching next-to-leading corrections with Parton Shower

In this Section we discuss the consistent inclusion of an exact fixed order calculation in a cross section resumming the leading corrections up to all orders of perturbation theory, in a QED Parton Shower (PS) approach. The algorithm described below is now implemented in the new version of the event generator **BABAYAGA** [27], at present only for the Bhabha process.

The matching of the two calculations is a non trivial task and it has to avoid the double counting at first order in α of the leading corrections already accounted for by the PS.

A general expression for the cross section with the emission of an arbitrary number of photons, in leading-log (LL) approximation, can be cast in the following form:

$$d\sigma_{LL}^{\infty} = \Pi(Q^2, \varepsilon) \sum_{n=0}^{\infty} \frac{1}{n!} |\mathcal{M}_{n,LL}|^2 d\Phi_n \quad (1)$$

where $\Pi(Q^2, \varepsilon)$ is the Sudakov form-factor accounting for the soft-photon (up to an energy equal to ε in units of the incoming fermion energy E) and virtual

emissions, ε is an infrared separator dividing soft and hard radiation and Q^2 is related to the energy scale of the process. $|\mathcal{M}_{n,LL}|^2$ is the squared amplitude in LL approximation describing the process with the emission of n hard photons, with energy larger than ε in units of E . $d\Phi_n$ is the exact phase-space element of the process (divided by the incoming flux factor), with the emission of n additional photons with respect to the Born-like final-state configuration: considering Bhabha scattering and defining p_1, p_2, p_3, p_4 and k_i ($i = 0, \dots, n$) as the initial-state e^- and e^+ , the final-state e^- and e^+ and photons' momenta respectively, $d\tilde{\Phi}_n \equiv d\Phi_n \times flux$ reads

$$d\tilde{\Phi}_n = \begin{cases} \frac{1}{(2\pi)^2} \frac{d^3\vec{p}_3}{2p_3^0} \frac{d^3\vec{p}_4}{2p_4^0} \delta^4(p_1 + p_2 - p_3 - p_4) & \text{if } n = 0 \\ \frac{1}{(2\pi)^{3n+2}} \frac{d^3\vec{p}_3}{2p_3^0} \frac{d^3\vec{p}_4}{2p_4^0} \delta^4(p_1 + p_2 - p_3 - p_4 - \sum_{i=1}^n k_i) \prod_{i=1}^n \frac{d^3\vec{k}_i}{2k_i^0} & \text{if } n > 0 \end{cases} \quad (2)$$

The cross section $d\sigma_{LL}^\infty$ of Eq. (1) is independent of the infrared separator ε , provided it is sufficiently small.

According to the factorization theorems of soft and/or collinear singularities, the squared amplitudes in LL approximation can be written in a factorized form. In the following, for the sake of clarity and without loss of generality, we write photon emission formulas as if only one external fermion radiates. We are aware that it is a completely unphysical case, but it allows to write more compact formulas, being the generalization to the real case straightforward when including the suited combinatorial factors. With this in mind, the one-photon emission squared amplitude in LL approximation can be written as

$$|\mathcal{M}_{1,LL}|^2 = \frac{\alpha}{2\pi} \frac{1+z^2}{1-z} I(k) |\mathcal{M}_0|^2 \frac{8\pi^2}{E^2 z(1-z)} \quad (3)$$

where $1-z$ is the fraction of the fermion energy E carried by the photon, k is the photon four-momentum, $I(k)$ is a function describing the angular spectrum of the photon and $P(z) = (1+z^2)/(1-z)$ is the Altarelli-Parisi $e \rightarrow e + \gamma$ splitting function. In Eq. (3) we observe the factorization of the Born squared amplitude and that the emission factor $\frac{\alpha}{2\pi} P(z) I(k) \frac{8\pi^2}{E^2 z(1-z)}$ can be iterated for each photon emission, up to all orders, to obtain $|\mathcal{M}_{n,LL}|^2$. It is worth noticing that $d^3\vec{k}/k^0 = (1-z)E^2 d\Omega_\gamma dz$ and that in the collinear limit the cross section of Eq. (1) reduces to the cross section calculated by means of the QED PS algorithm described in Refs. [12,13].

The Sudakov form factor $\Pi(Q^2, \varepsilon)$ reads explicitly

$$\Pi(Q^2, \varepsilon) = \exp\left(-\frac{\alpha}{2\pi} I_+ L'\right), \quad L' = \log \frac{Q^2}{m^2}, \quad I_+ \equiv \int_0^{1-\varepsilon} dz P(z) \quad (4)$$

The function $I(k)$ has the property that $\int d\Omega_\gamma I(k) = \log Q^2/m^2$ and allows the cancellation of the infrared logarithms.

The cross section calculated in Eq. (1) has the advantage that the photonic corrections, in LL approximation, are resummed up to all orders of perturbation theory. On the other side, the weak point of the formula (1) is that its expansion at $\mathcal{O}(\alpha)$ does not coincide with an exact $\mathcal{O}(\alpha)$ (NLO) result, being its LL approximation. In fact

$$\begin{aligned} d\sigma_{LL}^\alpha &= \left[1 - \frac{\alpha}{2\pi} I_+ \log \frac{Q^2}{m^2} \right] |\mathcal{M}_0|^2 d\Phi_0 + |\mathcal{M}_{1,LL}|^2 d\Phi_1 \\ &\equiv [1 + C_{\alpha,LL}] |\mathcal{M}_0|^2 d\Phi_0 + |\mathcal{M}_{1,LL}|^2 d\Phi_1 \end{aligned} \quad (5)$$

whereas an exact NLO cross section can be always cast in the form

$$d\sigma^\alpha = [1 + C_\alpha] |\mathcal{M}_0|^2 d\Phi_0 + |\mathcal{M}_1|^2 d\Phi_1 \quad (6)$$

The coefficient C_α contains the complete virtual $\mathcal{O}(\alpha)$ and the $\mathcal{O}(\alpha)$ soft-bremsstrahlung squared matrix elements, in units of the Born squared amplitude, and $|\mathcal{M}_1|^2$ is the exact squared matrix element with the emission of one hard photon. We remark that $C_{\alpha,LL}$ has the same logarithmic structure as C_α and that $|\mathcal{M}_{1,LL}|^2$ has the same singular behaviour of $|\mathcal{M}_1|^2$.

In order to match the LL and NLO calculations, we introduce the correction factors, which are by construction infrared safe and free of collinear logarithms,

$$F_{SV} = 1 + (C_\alpha - C_{\alpha,LL}), \quad F_H = 1 + \frac{|\mathcal{M}_1|^2 - |\mathcal{M}_{1,LL}|^2}{|\mathcal{M}_{1,LL}|^2} \quad (7)$$

and we notice that the exact $\mathcal{O}(\alpha)$ cross section can be expressed, up to terms of $\mathcal{O}(\alpha^2)$, in terms of its LL approximation as

$$d\sigma^\alpha = F_{SV} (1 + C_{\alpha,LL}) |\mathcal{M}_0|^2 d\Phi_0 + F_H |\mathcal{M}_{1,LL}|^2 d\Phi_1 \quad (8)$$

Driven by Eq. (8), Eq. (1) can be improved by writing the resummed cross section as

$$d\sigma_{matched}^\infty = F_{SV} \Pi(Q^2, \varepsilon) \sum_{n=0}^{\infty} \frac{1}{n!} \left(\prod_{i=0}^n F_{H,i} \right) |\mathcal{M}_{n,LL}|^2 d\Phi_n \quad (9)$$

The correction factors $F_{H,i}$ follow from the definition Eq. (7) for each photon emission. The expansion at $\mathcal{O}(\alpha)$ of Eq. (9) coincides now with the exact NLO

cross section Eq. (6) and all higher order LL contributions are the same as in Eq. (1).

Eq. (9) is our master formula for the matching between the exact $\mathcal{O}(\alpha)$ calculation and the QED resummed PS cross section, according to which we also generate events. The extension of the matching formula Eq. (9) to the realistic case, where every charged particle radiates photons, is almost straightforward. We would like to remark also that the LL cross section of Eq. (1) is by construction positively defined in every point of the phase space, whereas the correction factors of Eq. (7) can in principle make the differential cross section of Eq. (9) negative in some point, namely where the PS approximation is less accurate (e.g. for hard photons at large angles). Nevertheless, we verified that this never happens when considering typical event selection criteria for luminosity at flavour factories.

It is useful to present, in the realistic case, the expression of the function $I(k)$, which describes the leading behaviour of the angular spectrum of the emitted photons, accounting also for interference of radiation coming from different charged particles:

$$I(k) = \sum_{i,j=1}^4 \eta_i \eta_j \frac{p_i \cdot p_j}{(p_i \cdot k)(p_j \cdot k)} E_\gamma^2 \quad (10)$$

where p_l is the momentum of the external fermion l , η_l is a charge factor equal to +1 for incoming particles or outgoing antiparticles and equal to -1 for incoming antiparticles or outgoing particles, k is the photon momentum, E_γ is its energy and the sum runs over all the external fermions. The function $I(k)$ does not depend on the photon energy. Given Eq. (10), one can quite easily convince that the more convenient choice for the Sudakov form factor scale Q^2 is $L' = \log \frac{Q^2}{m^2} = \log \frac{st}{um^2} - 1 \equiv L - 1$ where s , t and u are the Mandelstam variables of the process and m is the electron mass.

The exact squared amplitude for the emission of a real photon $|\mathcal{M}_1|^2$ has been calculated by hand with the help of FORM [28] and successfully cross checked with Ref. [16] and with the output of the ALPHA algorithm [29].

The exact $\mathcal{O}(\alpha)$ soft plus virtual corrections to the Bhabha scattering have been taken from Ref. [30]. The soft plus virtual cross section reads

$$\begin{aligned} d\sigma_{SV}^\alpha &= d\sigma_{SV}^{\alpha,s} + d\sigma_{SV}^{\alpha,t} + d\sigma_{SV}^{\alpha,st} \\ d\sigma_{SV}^{\alpha,i} &= d\sigma_0^i [2(\beta + \beta_{int}) \log \varepsilon + C_F^i] \end{aligned} \quad (11)$$

where i is an index for s , t and s - t subprocesses contributing to the Bhabha cross section, $\beta = \frac{2\alpha}{\pi} [\log(s/m^2) - 1]$, $\beta_{int} = \frac{2\alpha}{\pi} \log(t/u)$ and the explicit ex-

pression for C_F^i can be found in Ref. [30]. We notice that in Eq. (11) the terms coming from s , t and s - t interference diagrams are explicitly given.

In the following, we discuss the implementation of the vacuum polarization effects in BABAYAGA. Some technical aspects about Eq. (9) (its independence from ε , the mapping of the momenta needed for $n \geq 2$ and the importance sampling of the final-state collinear singularities) are discussed in Appendix A.

2.1 Vacuum polarization and Z exchange contributions

Besides the photonic radiative corrections considered in the previous Section, also the vacuum polarization effects must be included in the master formula (9), in order to reach the required theoretical accuracy. They are accounted for by replacing the fine structure constant $\alpha \equiv \alpha(0)$ with $\alpha(q^2) = \alpha/(1 - \Delta\alpha(q^2))$, where $\Delta\alpha(q^2)$ is the fermionic contribution to the photon self-energy: the leptonic and top-quark one-loop contributions can be calculated analytically in perturbation theory, while the remaining five quarks (hadronic) contribution, $\Delta\alpha_{had}^{(5)}$, has to be extracted from data. To evaluate $\Delta\alpha_{had}^{(5)}$ we use the HADR5N routine by F. Jegerlehner [3,31].

Setting $r_s = \alpha(s)/\alpha$ and $r_t = \alpha(t)/\alpha$ (s and t are the Mandelstam invariants), we include vacuum polarization in the Born matrix element, which is proportional to α , by rescaling the s and t channel amplitudes, namely

$$|\mathcal{M}_0|^2 = |\mathcal{M}_{0,s} + \mathcal{M}_{0,t}|^2 \quad \rightarrow \quad |\mathcal{M}_{0,VP}|^2 = |\mathcal{M}_{0,s}r_s + \mathcal{M}_{0,t}r_t|^2 \quad (12)$$

Going beyond the Born-like approximation, the cross section corrected at $\mathcal{O}(\alpha)$ including also vacuum polarization can be written as $\sigma_{VP}^\alpha = \sigma_{0,VP} + \sigma_{SV}^\alpha + \sigma_H^\alpha$, where σ_{SV}^α and σ_H^α are the soft plus virtual and the hard photon $\mathcal{O}(\alpha)$ corrections of photonic origin. We can go a step further and include vacuum polarization in those terms, in order to include also part of the $\mathcal{O}(\alpha^2)$ factorizable corrections. The hard emission matrix element is the sum of eight amplitudes where the real photon is attached to a s or t channel-like diagram. As in Eq. (12), we rescale those amplitudes by r_s and r_t , respectively. In order to guarantee the cancellation of the infrared separator ε between σ_{SV}^α and σ_H^α , also in σ_{SV}^α of Eq. (11), we rescale the s , t and s - t interference contributions with the appropriate vacuum polarization factor, namely r_s^2 , r_t^2 and $r_s r_t$. Finally, the vacuum polarization improved amplitudes and cross sections are used as building blocks of the master formula (9).

Furthermore, we add to the Born amplitude also the Z exchange diagrams: their effect is really tiny and negligible at low energies, but can become more

important (up to 0.1%) around 10 GeV when considering wide angular acceptance regions.

3 Numerical results

In order to test the internal consistency of the formulation described above and to quantify the physical precision of the improved version of the BABAYAGA generator, we performed a number of Monte Carlo simulations of those experimental observables which are relevant for luminosity measurements at e^+e^- flavour factories. To model the acceptance cuts used by the experimental collaborations, we considered four different set up defined by the following selection criteria

- (a) $\sqrt{s} = 1.02$ GeV, $E_{min} = 0.408$ GeV, $20^\circ < \theta_\pm < 160^\circ$, $\xi_{max} = 10^\circ$
- (b) $\sqrt{s} = 1.02$ GeV, $E_{min} = 0.408$ GeV, $55^\circ < \theta_\pm < 125^\circ$, $\xi_{max} = 10^\circ$
- (c) $\sqrt{s} = 10$ GeV, $E_{min} = 4$ GeV, $20^\circ < \theta_\pm < 160^\circ$, $\xi_{max} = 10^\circ$
- (d) $\sqrt{s} = 10$ GeV, $E_{min} = 4$ GeV, $55^\circ < \theta_\pm < 125^\circ$, $\xi_{max} = 10^\circ$

where $E_{min} = 0.8 \times E_{beam}$ is the energy threshold for the final-state electron/positron, θ_\pm are the electron/positron scattering angles and ξ_{max} is the maximum allowed acollinearity. The set up (a) and (b) are of interest for Φ factories, while set up (c) and (d) refer to B -factories. In both cases, a wider and a tighter angular acceptance are considered, in order to study the dependence of the radiative corrections from the acceptance criteria. The energy and acollinearity cuts are very similar to those considered in previous simulations and tend to single out quasi-elastic Bhabha events. It is understood that the energy of final-state electron/positron corresponds to a so-called “bare” event selection (i.e. without photon recombination), which resembles realistic data taking at flavour factories.

3.1 Integrated cross sections and technical tests

A first meaningful test of the correct matching of NLO corrections with PS is to prove independence of the predictions for the QED corrected cross section from variation of the soft-hard separator ε required by the PS algorithm. This is successfully demonstrated in Fig. 1, which shows the Bhabha cross section, obtained according to Eq. (9) and in the conditions of set up (b), as a function of ε from 10^{-3} to 10^{-7} . A priori, one should expect compatibility of the calculated cross section against ε variation at an accuracy level of $\mathcal{O}(\alpha\varepsilon)$. This is clearly seen to be valid in Fig. 1, when looking at the relative difference between the cross section predictions as ε varies. Also for the $\mathcal{O}(\alpha)$ corrected

cross section, which is an important ingredient of the present formulation and a component of the following discussion, independence from ε has been successfully checked in the limit of sufficiently small values, i.e. for ε variations in the range $10^{-3} - 10^{-7}$.

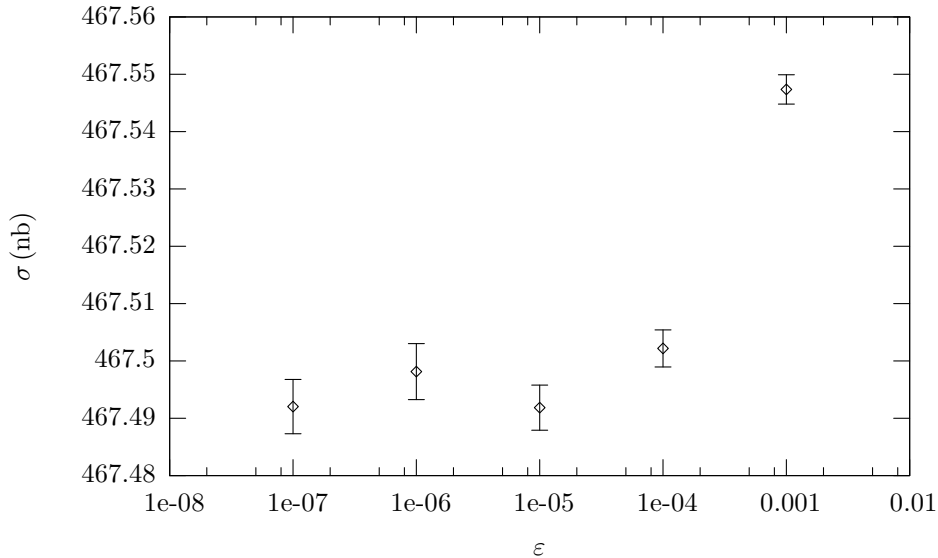


Fig. 1. QED corrected Bhabha cross section as a function of the infrared regulator ε , according to set up (b). The error bars correspond to 1σ Monte Carlo error.

To quantify the overall impact of QED radiation and, in particular, to evaluate the size of QED contributions at different perturbative/precision levels, we show in Tab. 1 the lowest-order Bhabha cross section (without and with vacuum polarization), the exact $\mathcal{O}(\alpha)$ cross section as in Eq. (6) and the $\mathcal{O}(\alpha)$ PS cross section as in Eq. (5), as well as the all-order PS cross section of Eq. (1) and the matched PS cross section of Eq. (9). The four columns correspond to the experimental conditions previously defined. In the cross sections of Tab. 1, we switch off the vacuum polarization effect except in the second row, to better study the different sources of corrections. Interestingly, from these cross section values it is possible to disentangle the relative effect of various QED contributions, namely the contribution of vacuum polarization, of exact $\mathcal{O}(\alpha)$ corrections, of higher-order (i.e. beyond $\mathcal{O}(\alpha)$) leading corrections in the pure PS approach and in the improved PS matched with $\mathcal{O}(\alpha)$ corrections, of non-logarithmic terms entering the $\mathcal{O}(\alpha)$ cross section and present also in the improved PS algorithm and, finally, of part of the sub-leading $\alpha^n L^{n-1}$ effects. The above per cent corrections are shown in Tab. 2 and they can be derived from the cross section values of Tab. 1 according to the following formulae

$$\delta_{VP} \equiv \frac{\sigma_{0,VP} - \sigma_0}{\sigma_0} \qquad \delta_\alpha \equiv \frac{\sigma_\alpha^{NLO} - \sigma_0}{\sigma_0}$$

$$\delta_{HO} \equiv \frac{\sigma_{matched}^{PS} - \sigma_\alpha^{NLO}}{\sigma_0} \qquad \delta_{HO}^{PS} \equiv \frac{\sigma^{PS} - \sigma_\alpha^{PS}}{\sigma_0}$$

$$\delta_{\alpha}^{non-log} \equiv \frac{\sigma_{\alpha}^{NLO} - \sigma_{\alpha}^{PS}}{\sigma_0} \quad \delta_{\infty}^{non-log} \equiv \frac{\sigma_{matched}^{PS} - \sigma^{PS}}{\sigma_0}$$

$$\delta_{\alpha^2L} \equiv \frac{\sigma_{matched}^{PS} - \sigma_{\alpha}^{NLO} - \sigma^{PS} + \sigma_{\alpha}^{PS}}{\sigma_0}$$

set up	(a)	(b)	(c)	(d)
σ_0	6855.743(1)	529.4631(2)	71.333(1)	5.5026(2)
$\sigma_{0,VP}$	6976.49(4)	542.657(6)	74.7632(6)	5.85526(3)
σ_{α}^{NLO}	6060.07 (6)	451.523 (6)	59.900 (1)	4.4256 (2)
σ_{α}^{PS}	6083.59 (6)	454.503 (6)	60.144 (1)	4.4565 (1)
$\sigma_{matched}^{PS}$	6086.74 (7)	455.858 (5)	60.419 (1)	4.5046 (3)
σ^{PS}	6107.57 (6)	458.437 (4)	60.628 (1)	4.5301 (2)

Table 1

Bhabha cross section (in nb) according to different precision levels and for the four set up specified in the text.

set up	(a)	(b)	(c)	(d)
δ_{VP}	1.76	2.49	4.81	6.41
δ_{α}	-11.61	-14.72	-16.03	-19.57
δ_{HO}	0.39	0.82	0.73	1.44
δ_{HO}^{PS}	0.35	0.74	0.68	1.34
δ_{α^2L}	0.04	0.08	0.05	0.10
$\delta_{\alpha}^{non-log}$	-0.34	-0.56	-0.34	-0.56
$\delta_{\infty}^{non-log}$	-0.30	-0.49	-0.29	-0.46

Table 2

Relative corrections (in per cent) to the Bhabha cross section for the four set up specified in the text.

From Tab. 2 it can be seen that the vacuum polarization gives a positive correction to the lowest-order cross section of the order of 2% at the Φ factories and of about 5-6% at the B factories, being its contribution more important for a tighter angular acceptance than for a wider one. This dependence of vacuum polarization from the detector acceptance has to be ascribed to the role played by the different sub-processes contributing to the Bhabha cross section as the angular acceptance varies. Actually, the energy scale entering the logarithmic dependence of the vacuum polarization is process dependent and is equal to the c.m. energy s for the time-like s -channel sub-process and to

(the absolute value of) the momentum transfer $|t|$ for the space-like t -channel contribution, being on the average $|t| \ll s$. While for a wide acceptance the t -channel contribution is largely dominating, the s -channel contribution becomes more and more important as the angular acceptance decreases, thus explaining the trend observed for the vacuum polarization correction. The exact $\mathcal{O}(\alpha)$ corrections lower the cross section of about 15% (Φ factories) and of about 20-25% (B -factories). Higher-order contributions of the type $\mathcal{O}(\alpha^n L^n)$, with $n \geq 2$, introduce a positive correction around 0.5-1% at the Φ factories and at the 1-2% level at the B factories. Therefore, multiple photon corrections are unavoidable in view of the required theoretical precision, as already noticed in Ref. [12]. On the other hand, also non-log $\mathcal{O}(\alpha)$ corrections are necessary at a precision level of 0.1%, since their contribution is of the order of 0.5%, almost independently from the c.m. energy and with a mild dependence from the angular cuts. This confirms *a posteriori* the need for matching the original PS formulation of BABAYAGA with NLO corrections. The effect due to $\mathcal{O}(\alpha^2 L)$ corrections varies from 0.05% (wide acceptance) to 0.1% (tight acceptance). Although these contributions are only approximately kept under control, it can be argued, and will be shown in the following Section, that the infrared part of $\mathcal{O}(\alpha^2 L)$ terms is correctly reproduced by the present approach [32] and, therefore, the size of such effects can be viewed as an estimate of the overall physical precision, which is conservatively close to 0.1%. From Tab. 2 it can be also seen that the matching of NLO corrections with PS does not alter at the level of 0.1% the size of higher-order and NLO contributions, thus preserving correctly the impact of these partial effects. This conclusion can be inferred by comparing δ_{HO} with δ_{HO}^{PS} and $\delta_{\alpha}^{non-log}$ with $\delta_{\infty}^{non-log}$, respectively. A common feature observed for all the relative corrections, with the exception of non-log effects, is the fact that, at a fixed c.m. energy, they are larger (by about a factor of two) for a tighter acceptance with respect to a wider one. This can be understood as follows. As discussed above, a natural choice for the Q^2 dependence of the collinear logarithm $L = \log Q^2/m^2$ is $Q^2 = st/u$. This implies that at large scattering angles the collinear logarithm tends to $\log s/m^2$, while for a wide angular acceptance it can be on the average approximated by $\log |t|/m^2$, thus explaining the observed angular-dependent behaviour.

3.2 Differential distributions

Besides the integrated cross section, various differential distributions are used by the experimental collaborations to monitor the collider luminosity. We show, in Fig. 2 and Fig. 3, two distributions which are particularly sensitive to the details of photon radiation, i.e. the e^+e^- acollinearity and the invariant mass distribution, in order to quantify the differences between the previous version of BABAYAGA (denoted as OLD in the figures) and the improved one

presented here (denoted as NEW). As a reference, the distributions obtained according to the exact $\mathcal{O}(\alpha)$ calculation are also shown. The results refer to set up (b).

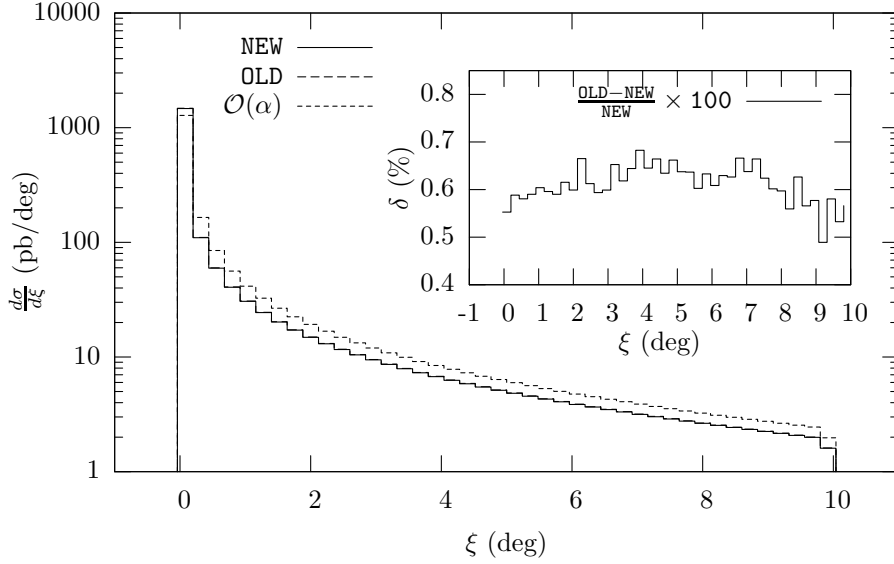


Fig. 2. Acollinearity distribution according to the PS matched with $\mathcal{O}(\alpha)$ corrections (Eq. (9), solid line), the LL PS algorithm (Eq. (1), dashed line) and the exact $\mathcal{O}(\alpha)$ calculation (dotted line). The inset shows the relative differences between the predictions of the improved and the LL PS. Selection criteria of set up (b) are considered.

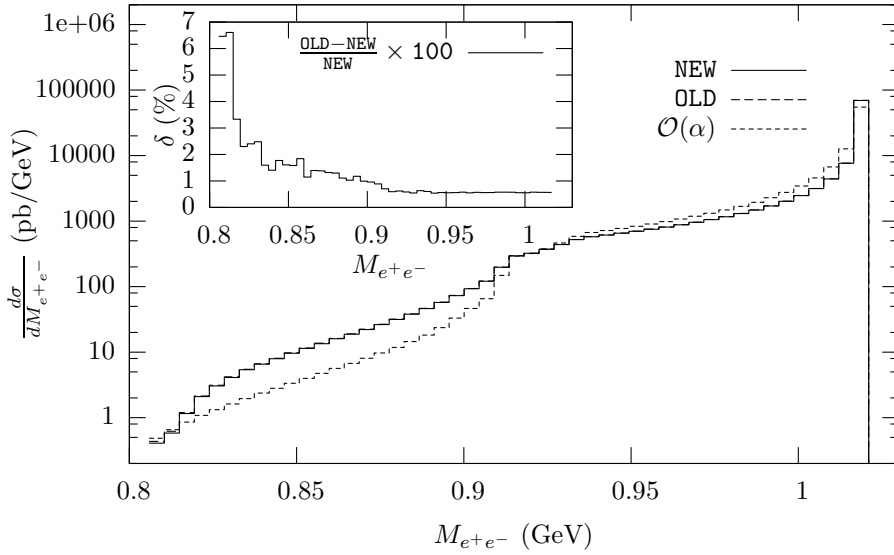


Fig. 3. The same as Fig. 2 for the e^+e^- invariant mass distribution.

From Fig. 2 and Fig. 3 it can be clearly seen that multiple photon corrections introduce significant deviations with respect to an $\mathcal{O}(\alpha)$ simulation, especially in the hard tails of the distributions, where they amount to several per cent. To make more visible the improvements introduced by the matching procedure discussed in Sect. 2, the inset shows the relative differences between the

predictions of the improved and original version of **BABAYAGA**. These differences mainly come from non-log $\mathcal{O}(\alpha)$ contributions and, to a smaller extent, from $\mathcal{O}(\alpha^2 L)$ terms. Their effect is flat and at level of 0.5% for the acollinearity distribution, while they reach the some per cent level in the hard tail of the invariant mass distribution. As a whole, these results demonstrate that exact $\mathcal{O}(\alpha)$ and higher-order corrections need to be simultaneously taken into account for precision luminosity studies.

3.3 Tuned comparisons

An important step towards the estimate of the theoretical accuracy of the formulation is the tuned comparison of the improved version of **BABAYAGA** with independent precision calculations of the Bhabha process. To this end, we first compared the results for the integrated cross section as obtained by the improved version of **BABAYAGA** with the corresponding predictions of **LABSPV** [33] and **BHWIDE** [17], which both rely on different theoretical ingredients. For the sake of comparison, the contribution of vacuum polarization has been switched off, in order to test just the implementation of pure QED corrections. The comparison is shown in Tab. 3, for both set up (a) and (b). As can be seen, the predictions of the three calculations agree within 0.1%. Although we didn't performed detailed tests in comparison with the recently developed generator **MCGPJ** [14], we expect a level of agreement with that calculation at a similar precision level, on the basis of the comparisons between **BHWIDE** and **MCGPJ** reported in Ref. [14].

set up	(a)	(b)
σ_{BHWIDE}	6086.3 (2)	455.73 (1)
σ_{LABSPV}	6088.5 (3)	456.19 (1)
$\sigma_{\text{BABAYAGA}}^{\text{matched}}$	6086.61 (2)	455.853 (4)

Table 3

Comparison between the predictions for the Bhabha cross section (in nb) as obtained with **BHWIDE**, **LABSPV** and the present version of **BABAYAGA**.

Comparisons between **BABAYAGA** and **BHWIDE** at the level of differential distributions are given in Fig. 4 and Fig. 5, where the inset shows the relative deviations between the predictions of the two codes, with reference to set up (b). As can be seen, there is a very good agreement between the two generators, as the predicted distributions appear, at a first sight, almost indistinguishable. Looking in more detail, there is a relative difference of a few per mille for the acollinearity distribution (Fig. 4) and of a few per cent for the invariant mass (Fig. 5), but only in the hard tails, which little contribute to the integrated cross section. In fact, these differences on differential distributions translate

into an agreement on the cross section values well below the 0.1% level, as shown in Tab. 3.

On the ground of these results, we can conclude that the calculation of QED corrections in the two generators, although based on different approaches, numerically agrees very well, at the level of the required precision for accurate luminosity measurements at flavour factories.

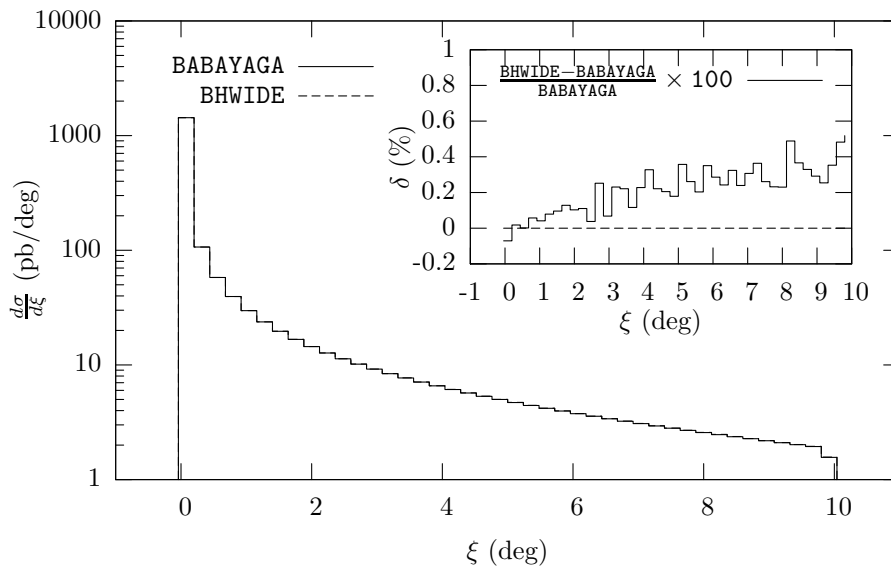


Fig. 4. Comparison between the BHWIDE generator (dashed line) and the present version of BABAYAGA (solid line) for the acollinearity distribution. The inset shows the relative difference between the predictions of the two generators. Selection criteria of set up (b) are considered.

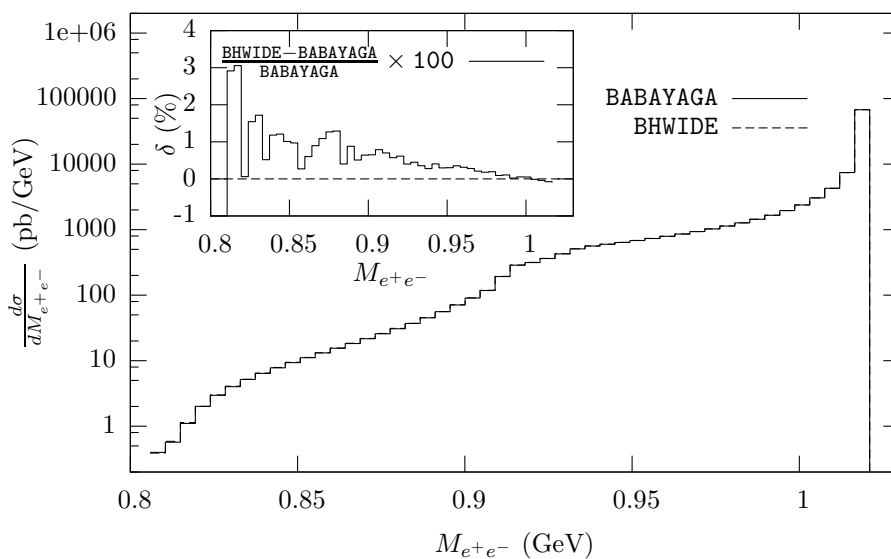


Fig. 5. The same as Fig. 4 for the e^+e^- invariant mass distribution.

4 Estimate of the theoretical accuracy

Since different implementations of radiative corrections beyond exact $\mathcal{O}(\alpha)$ contributions differ by higher order effects, the results of the comparisons quoted in the previous section between **BABAYAGA** and other event generators give a hint of the missing radiative corrections which dominate the theoretical accuracy. From the investigations of the previous Section, related to the higher order terms inherent in the theoretical formulation of **BABAYAGA** and to tuned comparisons with independent codes, an estimate of the physical precision in the calculation of the radiative corrections of the order of 0.1% can be inferred.

This guess can be verified by a comparison with a complete two-loop calculation, since all neglected terms in the formulation described in Sect. 2 start at two-loop order. Being a full two-loop calculation not presently available, the aim of the present Section is to try to estimate the impact of the uncertainties at order α^2 within the realistic set up considered in this paper, by comparing with some of the available calculations in the literature.

Another important source of error is the uncertainty on the hadronic contribution to the vacuum polarization $\Delta\alpha_{had}^{(5)}$, which will be quantified in Sect. 4.7. The origin of this error is intrinsically non-perturbative because $\Delta\alpha_{had}^{(5)}$ can not be calculated perturbatively around the hadronic resonances and must be calculated via dispersion relations by means of data [3]. As discussed in Sec. 4.7, this error will be the dominant one close to the J/Ψ resonances.

We start by considering the theoretical error of perturbative origin, at $\mathcal{O}(\alpha^2)$. The pure $\mathcal{O}(\alpha^2)$ content of our master formula (9) can be read by expanding it and can be cast in the following form

$$\sigma^{\alpha^2} = \sigma_{SV}^{\alpha^2} + \sigma_{SV,H}^{\alpha^2} + \sigma_{H,H}^{\alpha^2} \quad (13)$$

where $\sigma_{SV}^{\alpha^2}$ contains all the α^2 virtual and real contributions without photons with energy larger than ε , $\sigma_{SV,H}^{\alpha^2}$ contains all the virtual and real contributions with at least one photon with energy larger than ε and $\sigma_{H,H}^{\alpha^2}$ is the contribution with two real photons with energy larger than ε . In **BABAYAGA**, each of the three terms is affected in principle by an error and in the following we try to study the impact of this error on the integrated cross section to establish the theoretical accuracy of the master formula (9).

4.1 Corrections beyond two-loop

Before starting to discuss the theoretical error, we would like to prove that the LL radiative corrections beyond α^2 are still very important, at least when considering differential distributions. This means that even if the complete two-loop perturbative calculation will be fully available, it would be desirable a matching with the resummation of all the remaining LL corrections.

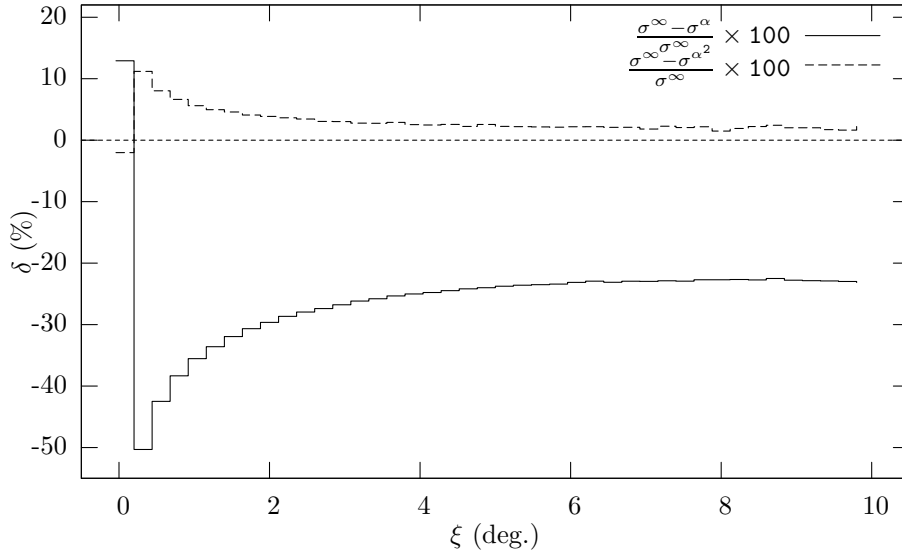


Fig. 6. Impact of α^2 (solid line) and higher order (dotted) corrections on the acollinearity distribution, in set up (b).

This can be demonstrated by comparing the fully resummed cross section of Eq. (9) with its expansion up to order α^2 , which, relying on the results of the next Sections, can be considered a really good approximation of the complete two-loop calculation. As in Sect. 3.3, here we switch off vacuum polarization effects.

In Fig. 6, the effect of the higher order corrections, dominated by α^3 contributions, is shown in comparison with that of the α^2 corrections on the acollinearity distribution for set up (b): as can be seen, the α^3 effect can be as large as 10% in the phase space region of soft photons emission, corresponding to small acollinearity angles with almost back-to-back final-state fermions.

4.2 Error on two real photons emission cross section

The cross section $\sigma_{H,H}^{\alpha^2}$ for the emission of two real photons in BABAYAGA is approximated by the integral over the phase space of $F_{1,H}F_{2,H}|\mathcal{M}_{2,LL}|^2d\Phi_2$. By means of the ALPHA [29] algorithm, the two real photon amplitude can be calculated exactly and then integrated over the (exact) phase space $d\Phi_2$. In

Tab. 4, the two real photons cross section as obtained with the approximation of Eq. (9) and with the exact matrix element are compared. We choose $\varepsilon = 1 \times 10^{-4}$ and we successfully verified that the difference of the cross sections Δ is independent of the ε choice, as expected. The error $\delta_{H,H}^{err}$ is measured in units of the Born cross section.

set up	$\sigma_{H,H}^{\alpha^2}$ (nb)	$\sigma_{\text{ALPHA}}^{\alpha^2}$ (nb)	Δ (nb)	$\delta_{H,H}^{err}$ (%)
(a)	2189.37(2)	2189.4(2)	-0.3(2)	$-4(3) \times 10^{-3}$
(b)	229.197(2)	229.20(2)	0.00(2)	$0(4) \times 10^{-4}$
(c)	44.0719(5)	44.072(5)	-0.00(5)	$0(7) \times 10^{-3}$
(d)	4.22839(4)	4.2286(5)	0.0002(5)	$4(9) \times 10^{-3}$

Table 4

Error on two real photon emission cross section.

In Tab. 4, we remark the small (and negligible) error, showing *a posteriori* that having corrected the real LL emissions with the factors $F_{H,i}$ in the master formula gives an extremely good approximation of the exact $\mathcal{O}(\alpha^2)$ squared amplitude, at least within the considered event selection criteria.

4.3 Light pair corrections

An $\mathcal{O}(\alpha^2)$ contribution which is not included in Eq. (13), even approximately, are the so-called pair corrections. Starting from the photonic one loop corrected diagrams, the virtual pair diagrams can be obtained by inserting a fermion loop in the correcting photon propagator. In order to estimate the size of the virtual pair corrections (VPC), we use the formulae of Ref. [34] (approximated at LL accuracy), for t channel Bhabha. VPC develop terms of the order of $\alpha^2 L^3$ which are then cancelled when also the real pair emissions (RPC) are included. We also estimate the size of the real pairs using the soft approximation of Ref. [35,36] and setting the maximum pair energy $\Delta E = 0.2 \times \sqrt{s}$, which is compatible with the requirements of set up (a)–(d) for the energy of the final-state leptons. In Tab. 5, the virtual and real pair cross section are reported, and the errors δ_{pairs}^{err} due to missing them in BABAYAGA is measured in units of the Born cross section. It is worth noting that the relative contribution of light pairs emission is at the level of a few 0.01%.

Here we consider only electron pairs. The contribution of muon pairs and hadronic pairs is expected to be one order of magnitude smaller with respect to electron pair production. This problem was investigated in Ref. [37] for the small angle Bhabha scattering at LEP1, where the typical momentum

set up	$\sigma_{VPC}^{\alpha^2}$ (nb)	$\sigma_{RPC}^{\alpha^2}$ (nb)	δ_{pairs}^{err} (%)
(a)	-4.605(3)	3.305(3)	-0.019
(b)	-0.5698(1)	0.4375(1)	-0.025
(c)	-0.1385(1)	0.1154(1)	-0.032
(d)	-0.01542(1)	0.01320(1)	-0.040

Table 5

Error due to the virtual and real electron pair corrections.

transfer is of the order of the energies involved at flavour factories. In Ref. [37] the global effect of muon and hadronic pairs was safely estimated at the level of 30% of the contribution of electronic pairs.

4.4 Comparisons with virtual plus soft two-loop calculations

In order to establish the error on $\sigma_{SV}^{\alpha^2}$ of Eq. (13), we compare it with recent calculations appeared in the literature. As mentioned in the introduction, there has been important progress towards the calculation of the full QED two-loop corrections (NNLO) to Bhabha scattering. An exhaustive report of the status of the two-loop QED corrections to Bhabha scattering can be found in Ref. [19]. What is actually available is the complete two-loop virtual photonic correction in the approximation of neglecting $\mathcal{O}(m^2/Q^2)$, where Q^2 stands for one of the Mandelstam invariants s , t and u [21]. The real radiation contribution is treated in the soft photon approximation and the calculation is differential in the electron scattering angle. The results have been confirmed by independent calculations [20,23]. In Ref. [23] the electron mass terms have been included but the two-loop box diagrams have been neglected. Work is in progress towards the calculation of massive two-loop box diagrams [24]. Another ingredient towards the two-loop complete calculation is the virtual fermionic contribution $N_f = 1$ [22] including all finite fermion mass effects. In Ref. [23] also real pair production [35] and photon emission in the soft limit have been introduced verifying the cancellation of infrared singularities as well as terms proportional to L^3 between virtual and real corrections.

We remark that, in order to achieve a NNLO accuracy in Bhabha scattering, also the exact two real photons corrections and the exact one-loop corrections to the one real photon emission process must be included [36,38]. The complete calculation of the latter in particular is still missing in the literature for the large-angle Bhabha scattering.

The cross section $\sigma_{SV}^{\alpha^2}$ of Eq. (13) can be directly compared with the results of Ref. [21,22,23], in order to quantify the size of the missing terms. In the following subsections the uncertainties inherent to the classes of pure photonic

and $N_f = 1$ corrections are separately investigated numerically.

As a first step we write explicitly $\sigma_{SV}^{\alpha^2}$, which is derived from the first term ($n = 0$) of the infinite sum in Eq. (9). In order to show the s , t and interference contributions, we define

$$\begin{aligned} d\sigma_{SV}^{\alpha} &= d\sigma_{s,SV}^{\alpha} + d\sigma_{t,SV}^{\alpha} + d\sigma_{st,SV}^{\alpha} \equiv (E_s + E_t + E_{st})d\sigma_0 \\ d\sigma_0 &= d\sigma_{s,0} + d\sigma_{t,0} + d\sigma_{st,0} \equiv (B_s + B_t + B_{st})d\sigma_0 \end{aligned} \quad (14)$$

Truncating every factor in Eq. (9), improved with vacuum polarization effects as described in Sect. 2.1, at $\mathcal{O}(\alpha^2)$ we get

$$\begin{aligned} \frac{d\sigma_{SV}}{d\sigma_0} &\simeq \left(1 + V + \frac{V^2}{2} \right) \\ &\times \left[1 + (E_s - VB_s)r_s^2 + (E_t - VB_t)r_t^2 + (E_{st} - VB_{st})r_s r_t \right] \\ &\times \left(B_s r_s^2 + B_t r_t^2 + B_{st} r_s r_t \right) \end{aligned} \quad (15)$$

where $V = -(2\alpha/\pi)I_+L'$ is the $\mathcal{O}(\alpha)$ term of the Sudakov form factor, E_i and B_i have been defined above and $r_{s,t}$ are the vacuum polarization corrections (including only electron loop to be consistently compared with the $N_f = 1$ results) for the s and t channels. If we define $1/(1 - \Delta\alpha(q^2)) \equiv 1/(1 - \delta_{q^2})$, r_s^2 , r_t^2 and $r_s r_t$ read:

$$\begin{aligned} r_s^2 &= 1 + 2\delta_s + 3\delta_s^2 \\ r_t^2 &= 1 + 2\delta_t + 3\delta_t^2 \\ r_s r_t &= 1 + \delta_s + \delta_t + \delta_s^2 + \delta_t^2 + \delta_s \delta_t \end{aligned} \quad (16)$$

We would like to stress that δ_i are calculated at one-loop order.

Retaining only terms up to $\mathcal{O}(\alpha^2)$, Eq. (15) reads

$$\begin{aligned} \frac{d\sigma_{SV}}{d\sigma_0} &= 1 \\ &+ V + (E_s - VB_s) + (E_t - VB_t) + (E_{st} - VB_{st}) \\ &+ 2(B_s\delta_s + B_t\delta_t) + B_{st}(\delta_s + \delta_t) \\ &+ 1/2V^2 \\ &+ (E_s - VB_s)\delta_s + (E_t - VB_t)\delta_t + (E_{st} - VB_{st})(\delta_s + \delta_t) \\ &+ 3(B_s\delta_s^2 + B_t\delta_t^2) + B_{st}(\delta_s^2 + \delta_t^2 + \delta_s\delta_t) \\ &+ V[(E_s - VB_s) + (E_t - VB_t) + (E_{st} - VB_{st})] \\ &+ V[2(B_s\delta_s + B_t\delta_t) + B_{st}(\delta_s + \delta_t)] \\ &+ [(E_s - VB_s) + (E_t - VB_t) + (E_{st} - VB_{st})] \times \end{aligned}$$

$$\times [2(B_s\delta_s + B_t\delta_t) + B_{st}(\delta_s + \delta_t)] \quad (17)$$

The first line of the previous equation is the Born contribution, the second line is the photonic one loop soft plus virtual correction (notice that it is equal to $E_s + E_t + E_{st}$ because $B_s + B_t + B_{st} = 1$), the third line is the vacuum polarization correction at $\mathcal{O}(\alpha)$ and the remaining lines represent $\sigma_{SV}^{\alpha^2}$.

4.4.1 Two-loop photonic corrections

After switching off the terms coming from vacuum polarization contributions ($\delta_s = \delta_t = 0$), the pure $\mathcal{O}(\alpha^2)$ term of the above equation can be compared with the analytical spectrum of Ref. [21]. In fact the approximation $s, t, u \gg m^2$ is fulfilled for the event selections (a), (b), (c) and (d) considered in Sect. 3. Since all infrared terms are factorized, all differences between Eq. (17) and the calculation of Ref. [21] are not expected to be infrared sensitive, apart from spurious terms in Eq. (17) suppressed by coefficients of the order of m^2/Q^2 ². The infrared behaviour of the difference between Eq. (17) and the results of Ref. [21] can be seen in Fig. 7 (upper curve), where the infrared regulator has been allowed to scan over a range of ten orders of magnitude for set up (a). The dashed curve fitting the circles has the following expression:

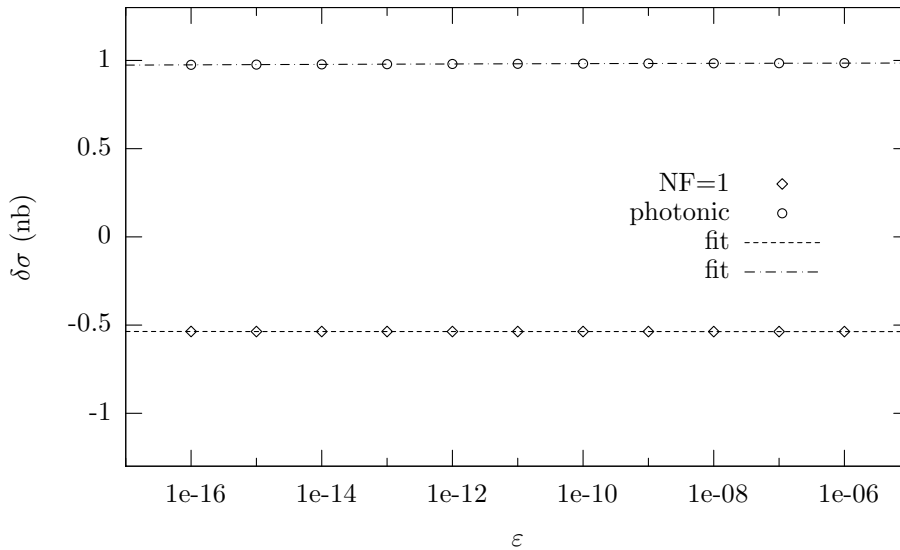


Fig. 7. Difference between the corrected cross section of Eq. (17) and the exact two loop photonic and $N_f = 1$ corrections, as a function of the infrared regulator ε , according to set up (a).

² In BABAYAGA, the terms proportional to m^2/Q^2 are only partially accounted for: for example, the fully massive kinematics is always considered, while the non-infrared $\mathcal{O}(m^2/Q^2)$ mass terms are neglected in the virtual one loop contributions.

$$\sigma_{SV}^{\alpha^2, \text{phot.}} - \sigma_{\text{Ref. [21]}}^{\alpha^2} = \left(\frac{\alpha}{\pi}\right)^2 \left(a \frac{m^2}{s} L^2 \log^2 \varepsilon + b \frac{m^2}{s} L^2 \log \varepsilon + cL \right) \sigma_0$$

$$a = -4.02 \pm 0.01$$

$$b = -6.7 \pm 0.4$$

$$c = +1.75447 \pm 0.00001 \quad (18)$$

with $\sigma_0 = 6855.7$ nb and $L = \log(s/m^2) = 15.2$. Equation (18) clearly demonstrates that in the difference infrared sensitive contributions survive, but are suppressed by the factor m^2/s . It also shows that, concerning photonic corrections, the error of BABAYAGA starts at the level of the $\alpha^2 L$ corrections, not enhanced by any infrared logarithm [32].

In order to numerically check that the term cL in Eq. (18) is a true single collinear logarithm, Fig. 8 shows a scan of the difference between the QED corrected Bhabha cross section of Eq. (17) and Ref. [21] (upper curve) as a function of the electron mass, whose values are allowed to span a range of eight orders of magnitude. The infrared regulator ε has been fixed to 1×10^{-5} . The dashed curve fitting the circles has the following expression:

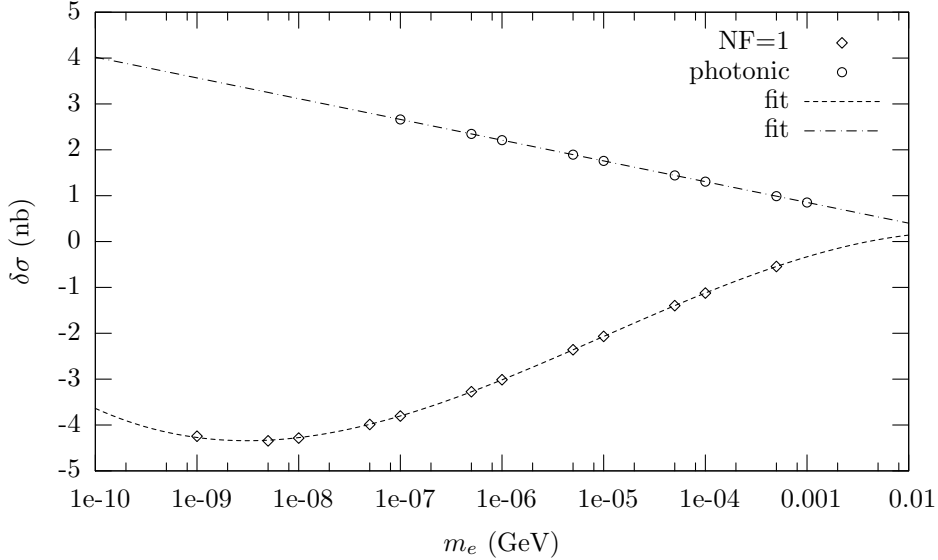


Fig. 8. Difference between the corrected cross section of Eq. (17) and the exact two loop photonic and $N_f = 1$ corrections, as a function of the electron mass, with the infrared regulator $\varepsilon = 1 \times 10^{-5}$, according to set up (a).

$$\sigma_{SV}^{\alpha^2, \text{phot.}} - \sigma_{\text{Ref. [21]}}^{\alpha^2} = \left(\frac{\alpha}{\pi}\right)^2 \left(a \log\left(\frac{s}{m^2}\right) + b\pi^2 \right) \sigma_0$$

$$a = +2.656 \pm 0.001$$

$$b = -1.391 \pm 0.003 \quad (19)$$

showing that the missing two-loop photonic contributions in BABAYAGA are

really of the order of $\alpha^2 L$. The impact on the integrated cross section within the realistic set up of these terms will be shown in Tab. 6.

4.4.2 Two-loop $N_f = 1$ corrections

The complete $N_f = 1$ virtual calculation of Ref. [22] refers to three types of diagrams: 1) diagrams with a fermionic loop in the tree-level photon propagator with a further photonic line within the loop; 2) diagrams with a fermionic loop in the photon propagators of the vertex and box one-loop diagrams; 3) diagrams with a fermionic loop in the tree-level diagrams with an additional photonic vertex correction. In the literature, type 2) diagrams are referred to as virtual pair corrections, while type 3) diagrams can be thought of as factorized in vacuum polarization times one-loop photonic correction contributions.

The part of $\sigma_{SV}^{\alpha^2}$ to be compared with two-loop $N_f = 1$ corrections is extracted from Eq. (17) by retaining all terms of photonic and vacuum polarization origin. In order to compare with the results of Ref. [23], we subtract from them the virtual pair corrections to the t -channel Bhabha scattering already considered in Sect. 4.3 ([34]). Furthermore, the soft real pair corrections included in Ref. [23] have been switched off, in order to perform a consistent comparison.

We expect that all infrared sensitive terms have the correct coefficient, owing to the factorization of infrared corrections, as can be seen in Fig. 7 (lower curve). The analytical expression of the dotted curve fitting the diamonds is given by

$$\begin{aligned} \sigma_{SV}^{\alpha^2, N_f=1} - [\sigma_{\text{Ref. [23]}}^{\alpha^2} - \sigma_{VPC}^{\alpha^2}] &= \left(\frac{\alpha}{\pi}\right)^2 \left(a \frac{m^2}{s} L^2 \log \varepsilon + bL\right) \sigma_0 \\ a &= -8.72 \pm 0.07 \\ b &= -0.955489 \pm 0.000006 \end{aligned} \tag{20}$$

showing that the two-loop $N_F = 1$ infrared structure in BABAYAGA is under control.

Concerning the dependence from the (logarithm of the) electron mass, apart from spurious coefficients of order m^2/Q^2 and a small residual $\alpha^2 L^3$ dependence due to VPC to s -channel Bhabha, the terms containing collinear logarithms have two sources, namely squared vacuum polarization and interference between vacuum polarization and photonic corrections. Thus the difference between $\sigma_{SV}^{\alpha^2, N_f=1}$ and the calculation of Ref. [23] (subtracted of the VPC of Sect. 4.3) should start from terms of the order of $\alpha^2 L^2$. In fact, the dotted curve fitting the diamonds of Fig. 8 has the following form:

$$\begin{aligned}
& \sigma_{SV}^{\alpha^2, N_f=1} - [\sigma_{\text{Ref. [23]}}^{\alpha^2} - \sigma_{VPC}^{\alpha^2}] = \\
& = \left(\frac{\alpha}{\pi}\right)^2 \left(a \log^3\left(\frac{s}{m^2}\right) + b \log^2\left(\frac{s}{m^2}\right) + c \log\left(\frac{s}{m^2}\right) + d\pi^2 \right) \sigma_0 \\
& a = +0.00728 \pm 0.00007 \\
& b = -0.504 \pm 0.005 \\
& c = +5.9 \pm 0.1 \\
& d = -1.36 \pm 0.08
\end{aligned} \tag{21}$$

In the next Section the size of the error induced by missing exact photonic and $N_f = 1$ corrections in $\sigma_{SV}^{\alpha^2}$ is discussed.

4.5 Error on purely virtual plus soft two-loop cross section

The numerical effect on the cross section, for the four different set up considered in this study, is shown in Tab. 6, with the infrared separator ε set to 10^{-5} . In Tab. 6, the Δ are the difference of the exact and the BABAYAGA α^2 virtual plus soft cross section and δ^{err} are their size in unit of the Born cross section. It is worth noticing the accidental opposite sign between δ_{phot}

set up	Δ_{phot} (nb)	$\Delta_{N_f=1}$ (nb)	δ_{phot}^{err} (%)	$\delta_{N_f=1}^{err}$ (%)	$\delta_{phot+N_f=1}^{err}$ (%)
(a)	0.9855	-0.537(2)	0.014	-0.0078	0.0062
(b)	0.1218	-0.0442(3)	0.023	-0.0083	0.0147
(c)	0.0149	-0.01436(4)	0.021	-0.020	0.001
(d)	0.0016	-0.00099(1)	0.029	-0.018	0.011

Table 6

Cross section difference ($\Delta_{phot, N_f=1}$) as obtained with $\sigma_{SV}^{\alpha^2}$ and the exact two loop corrections, for purely photonic contributions and $N_f = 1$. $\delta_{phot, N_f=1}$ are the differences of the cross sections in units of the Born one.

and $\delta_{N_f=1}$ for all event selections considered, allowing to reduce the error of BABAYAGA predictions when summing up everything together.

4.6 Error on the virtual plus soft corrections to one photon real emission

The virtual plus soft cross section with one hard photon $\sigma_{SV,H}^{\alpha^2}$ of Eq. (13) is obtained from the $\mathcal{O}(\alpha^2)$ content of the term $n = 1$ in Eq. (9). Its exact expression for large angle Bhabha scattering is not known in the literature, but it was calculated for the small angle Bhabha process [38] or for the s -channel [39] at large angles. Relying on the LEP experience and on the purely virtual plus soft results described in Sects. 4.4.1 and 4.4.2, the error of the

BABAYAGA approximation is at the level of the infrared-safe $\alpha^2 L$ terms, the size of which can be safely taken to be smaller than the 0.05% for all the set up.

4.7 Non-perturbative error induced by hadronic contribution to vacuum polarization

By means of the analysis presented in the previous Sections, we can deduce that the missing $\mathcal{O}(\alpha^2)$ (perturbative) contributions in BABAYAGA do not exceed the 0.1%.

Nevertheless, besides the missing $\mathcal{O}(\alpha^2)$ contributions considered before, another source of theoretical error, coming from the hadronic contribution to the vacuum polarization, has to be carefully considered. This uncertainty has an intrinsically non-perturbative origin. Since the routine HADR5N, by means of which we calculate $\Delta\alpha_{had}^{(5)}(q^2)$, returns also an error δ_{had} on its value, we estimate the induced error by computing the cross section with $\Delta\alpha_{had}^{(5)}(q^2) \pm \delta_{had}$ and taking the difference as the theoretical uncertainty due to the hadronic contribution to vacuum polarization. In Tab. 7, the uncertainties Δ are calculated for the event selection criteria (a)-(d) on the Born and the matched cross section. The quantities δ_{VP}^{err} are the errors in units of the Born cross section. Differently from previous investigations of vacuum polarization uncertainty in small-angle Bhabha scattering at LEP [40], we consider here only the error induced by the parameterization of hadronic loops of Refs. [3,31], because of the absence of other results able to keep under control appropriately the contribution of hadronic resonances for time-like momenta circulating in the photon self-energy.

set up	Δ_{Born} (nb)	Δ_{full} (nb)	$\delta_{VP,Born}^{err}$ (%)	$\delta_{VP,full}^{err}$ (%)
(a)	-0.48	-0.50	-0.007	-0.007
(b)	-0.00070	-0.0014	0.	0.
(c)	0.017	0.014	0.024	0.020
(d)	0.0033	0.0024	0.060	0.044

Table 7

Error induced by the uncertainty on $\Delta\alpha_{had}^{(5)}(q^2)$.

It must be remarked that the error on $\Delta\alpha_{had}^{(5)}(q^2)$ for $q^2 > 0$ strongly varies and increases passing through hadronic resonances. This yields a worsening of the theoretical accuracy of Bhabha cross section, in particular close to the $c\bar{c}$ states in the region between 3 and 4.5 GeV which have a non-negligible branching ratio into electrons. Relying on the output of the HADR5N routine (which here prints a warning about its reliability), we verified that the error

on the Bhabha cross section induced by hadronic loop may reach the 0.5% in this region and it is therefore the limiting factor for the theoretical accuracy.

4.8 Summary of the theoretical errors

The size of the α^2 contributions missing in **BABAYAGA** and the error induced by the hadronic contribution to the vacuum polarization, within the realistic event selection criteria considered in this paper, are summarized in Tab. 8.

$ \delta^{err} $ (%)	(a)	(b)	(c)	(d)
$ \delta_{VP}^{err} $	0.01	0.00	0.02	0.04
$ \delta_{pairs}^{err} $	0.02	0.03	0.03	0.04
$ \delta_{H,H}^{err} $	0.00	0.00	0.00	0.00
$ \delta_{phot+N_f=1}^{err} $	0.01	0.01	0.00	0.01
$ \delta_{SV,H}^{err} $	0.05	0.05	0.05	0.05
$ \delta_{total}^{err} $	0.09	0.09	0.10	0.14

Table 8

Summary of different source of theoretical error in **BABAYAGA**.

The size of the virtual and real pair corrections and of the missing virtual corrections to the real photon emission process is only guessed with a safe estimate of their impact. We also remark that the somehow large error coming from vacuum polarization uncertainty in set up (c) and (d) is due to the fact that we consider energies around the Υ resonance and the data-driven routine **HADR5N** produces here larger errors.

From Tab. 8, by summing up the absolute value of all the uncertainties, we can deduce that a safe estimate of the total theoretical accuracy of the new version of **BABAYAGA** (based on the master formula (9) and the **HADR5N** routine for the hadronic contribution to the vacuum polarization) for the calculation of the Bhabha cross section is 0.1% at Φ factories and below 0.2% at the B factories.

We remark that concerning the perturbative $\mathcal{O}(\alpha^2)$ error, our formulation is able to reach the 0.1% accuracy in all the considered set up and that, as previously emphasized, the accuracy can be worsened to the 0.5% level in proximity of the J/Ψ resonances because of the error on the non-perturbative hadronic contribution to the vacuum polarization.

5 Conclusions

Bhabha scattering is a crucial process for precise luminosity monitoring of e^+e^- colliders. Ongoing and future experiments at e^+e^- accelerators operating in the region of hadronic resonances, such as Φ , τ -charm and B factories, require a precise luminosity knowledge, especially in view of improved measurements of the hadronic cross section in the energy region going from the pion pair production threshold up to 12 GeV.

With this motivation in mind, we have presented in this paper a high-precision calculation of the Bhabha process in QED, with a precision target of the order of 0.1%. This theoretical accuracy is achieved by the matching of exact NLO corrections with higher-order leading logarithmic contributions, which are kept under control through all orders of α by means of a QED Parton Shower approach. The matching of matrix element corrections with Parton Showers is a topic of QCD calculations and recently different successful solutions have been proposed, opening the way towards precision calculations of high-energy QCD processes [41]. Our matching algorithm represents, to the best of our knowledge, the first example of such an application in QED. The theoretical precision of the approach has been demonstrated through detailed comparisons with the predictions of precise independent generators and, noticeably, with the results of recent calculations of two-loop corrections to Bhabha process, which are the frontier of modern perturbative QED. Other components of the theoretical luminosity error, coming from hadronic vacuum polarization and light pair emission, has been carefully estimated as well, in order to arrive at a sound and robust total error budget. In particular, the perturbative contribution to the error coming from missing $\mathcal{O}(\alpha^2)$ corrections has been shown to be under control at the 0.1% level for all the experimental selection criteria here considered, realistic for data analysis at flavour factories. Furthermore, the non-perturbative error due to the uncertainty on the hadronic contribution to vacuum polarization, which critically depends on the centre-of-mass energy, turns out to be below the 0.05% level at Φ and B factories, whereas can increase up to the 0.5% in proximity of the $c\bar{c}$ bound states. The reduction of such an uncertainty, if needed, requires progress both on the theory and the experimental side.

The theoretical precision for luminosity monitoring through large-angle Bhabha scattering at flavour factories is now comparable with the accuracy reached at the time of the LEP workshop working groups 95/96 for the theoretical error underlying the high-precision small-angle Bhabha measurement at LEP [40,42].

The new formulation has been implemented in an improved version of the event generator BABAYAGA [27], which is available for high-precision luminosity

measurements at flavour factories. For example, this will allow to reduce the theoretical error in the luminosity measurement at the Φ factory DAΦNE from the present 0.5% to 0.1%, thus roughly halving the total luminosity error quoted by KLOE collaboration at DAΦNE and, more generally, paving the road to more precise measurements of the Bhabha process at other e^+e^- collider, such as BEPC, CESR, KEK-B, PEP-II and VEPP-2M.

As far as possible future applications of the approach here presented are concerned, it would certainly be of interest for future data analysis extending the present phenomenological analysis to the production processes of muon and photon pairs in e^+e^- annihilation, as well as to their exclusive signatures such as $e^+e^- \rightarrow \mu^+\mu^-\gamma$, because also these QED reactions are employed at flavour factories for precise luminosity studies [1]. Other interesting perspectives would be the applying the matching procedure to the Standard Model processes presently under consideration for luminosity monitoring of a future e^+e^- collider at the TeV scale and extending the matching to incorporate also the full two-loop corrections.

These developments are by now under consideration.

Acknowledgments

We are grateful to M. Moretti for the help in the use of the ALPHA code and for many useful discussions and to R. Bonciani, A. Ferroglia and A. Vicini for having carefully read the preliminary manuscript. We are indebted with R. Bonciani, A. Ferroglia and A. Penin for providing us the numerical program implementing the two-loop calculations. We also wish to thank A. Denig, S. Eidelman, F. Jegerlehner, F. Nguyen and G. Venanzoni for many informative discussions and continuous interest in our work.

A Technical details

Here we discuss some technical details about Eq. (9) and its integration, namely the independence from ε , the mapping of the momenta needed for $n \geq 2$ and the importance sampling of the final-state collinear singularities.

A.1 Independence of the master formula from the infrared separator

Considering Eq. (1), its independence from ε can be demonstrated analytically if we neglect the variation of $|\mathcal{M}_0|^2$ from the center of mass energy. In this case, integrating over all the phase space, we get

$$\sigma \simeq \exp\left(-\frac{\alpha}{2\pi}I_+L'\right) \sum_{n=0}^{\infty} \left(\frac{\alpha}{2\pi}\right)^n L'^n I_+^n \sigma_0 = \sigma_0 \quad (\text{A.1})$$

Considering now Eq. (9), we can write the integral of the radiation factor for each emitted photon as $\frac{\alpha}{2\pi}L'(I_+ + c)$, where c is a constant not singular as ε goes to zero and coming from the correction factor F_H . Thus, the total cross section can be written as

$$\begin{aligned} \sigma &\simeq F_{SV} \exp\left(-\frac{\alpha}{2\pi}I_+L'\right) \sum_{n=0}^{\infty} \left(\frac{\alpha}{2\pi}\right)^n L'^n (I_+ + c)^n \sigma_0 \\ &= F_{SV} \exp\left(\frac{\alpha}{2\pi}c\right) \sigma_0 \end{aligned} \quad (\text{A.2})$$

which does not depend on ε . It is worth noticing that having corrected each hard photon emission in Eq. (9) with the factors $F_{H,i}$ is crucial for the good infrared behaviour of the integrated cross section. In Fig. 1 of Sect. 3 the numerical independence from the infrared separator has been shown.

A.2 Mapping of the momenta for $n \geq 2$

In the master formula (9), the sum over all possible photon multiplicities is required, but the building blocks of the matched cross section (i.e. the squared matrix elements) are strictly defined only for 0 or 1 photon in the final state. It is therefore mandatory to devise an algorithm to map a n photons momenta configuration to a 0 or 1 photon configuration in order to consistently calculate the squared amplitudes $|\mathcal{M}_0|^2$ and $|\mathcal{M}_1|^2$. The mapping algorithm is not unique, but the choice among different mappings gives a higher order effect which has been verified to be negligible.

When a photon multiplicity n is selected, the first step to define a zero-photon kinematics configuration is to associate n_I photons as emitted by the initial state and n_F by the final state. The association is done according to an algorithm finding whether the photon is nearer to an initial-state or final-state fermion, in terms of its angle with respect to the fermion. If $K_I = \sum_{j=1}^{n_I} k_j$ and $q = p_1 + p_2 - K_I$, two initial-state mapped momenta are defined such as

$(p_{1,M} + p_{2,M})^2 = q^2$ and $p_{1,M}^2 = p_{2,M}^2 = m^2$. The mapped final-state momenta are defined such as $(p_{3,M} + p_{4,M})^2 = (p_{1,M} + p_{2,M})^2$, $p_{3,M}^2 = p_{4,M}^2 = m^2$ and $p_{3,M}$ is directed along the direction of p_3 boosted in the frame where $p_3 + p_4$ is at rest. The mapped momenta, which satisfy by construction momentum conservation and on-shell relations, are used to calculate the Lorentz-invariant Born squared amplitude needed to compute $|\mathcal{M}_{n,LL}|^2$ in Eq. (9).

In order to calculate the correction factors $F_{H,i}$, a mapping to 1 photon configuration is needed. Suppose we are calculating $F_{H,l}$ for the l -th photon: in order to get the mapped momenta, we do as if only this photon is present. We keep $p_{1,M} = p_1$, $p_{2,M} = p_2$ and $k_{l,M} = k_l$, we boost p_3 and p_4 where $p_3 + p_4$ is at rest, we calculate $p_{3,M}$ and $p_{4,M}$ such as $(p_{3,M} + p_{4,M})^2 = (p_{1,M} + p_{2,M} - k_{l,M})^2$, $p_{3,M}^2 = p_{4,M}^2 = m^2$ and $p_{3,M}$ is directed along p_3 in this frame and finally we boost $p_{3,M}$ and $p_{4,M}$ back in the original frame. We obtain a set of mapped momenta satisfying momentum conservation and on-shell relations which can be used to calculate $|\mathcal{M}_1|^2$ and $|\mathcal{M}_{1,LL}|^2$ and the correction factors $F_{H,i}$.

A.3 Importance sampling of final-state collinear singularities

The integral over the phase space $d\Phi_n$ is done by means of Monte Carlo techniques. For n photons in the final state, the number of independent integration variables is $3n + 2$, and we choose them to be the azimuthal and the polar angles of one of the final-state fermions and the energies and the angles of the n emitted photons. With this choice, $d\tilde{\Phi}_n \equiv d\Phi_n \times flux$ can be written as

$$d\tilde{\Phi}_n = \frac{k_1^0 \cdots k_n^0}{(2\pi)^{3n+2} 2^{n+2}} \frac{|\vec{p}_3|}{p_4^0 + p_3^0 \left(1 + \frac{\vec{K} \cdot \vec{p}_3}{|\vec{p}_3|^2}\right)} dk_1^0 \cdots dk_n^0 d\Omega_{\gamma_1} \cdots d\Omega_{\gamma_n} d\Omega_3 \quad (\text{A.3})$$

where $K \equiv \sum_{i=1}^n k_i$ and the final-state momenta are easily calculated with the independent variables by requiring momentum conservation and on-shell relations. In Eq. (A.3), the angles of the final-state electron have been chosen, but the positron could have been equivalently chosen.

The generation of the independent variables is done according to the peaking structure of the function to be integrated. Here we discuss in some detail the sampling of the final-state collinear singularities. The peaks of the differential cross section can be read from $|\mathcal{M}_{n,LL}|^2 d\Phi_n$ (the correction factors $F_{H,i}$ tend to 1 in the singular regions), namely

$$|\mathcal{M}_{n,LL}|^2 d\Phi_n \propto dk_1^0 \cdots dk_n^0 d\Omega_{\gamma_1} \cdots d\Omega_{\gamma_n} d\Omega_3 \frac{1}{k_1^0 \cdots k_n^0} I(k_1) \cdots I(k_n) \quad (\text{A.4})$$

In the previous equation the infrared and collinear singularities for each emitted photon are evident. If infrared singularities do not present problems (photon energies have to be sampled as $1/k^0$), collinear peaks, appearing in $\prod_{i=1}^n I(k_i)$, have to be carefully treated when $n \geq 2$.

Firstly, $\prod_{i=1}^n I(k_i)$ is flattened with the function $\prod_{i=1}^n \tilde{I}(k_i)$, where $\tilde{I}(k) \equiv \sum_{i=1}^4 \frac{1}{p_i \cdot k}$ has the same leading singularities of the original function. We then write

$$\begin{aligned} \prod_{i=1}^n I(k_i) &= \prod_{i=1}^n \frac{I(k_i)}{\tilde{I}(k_i)} \tilde{I}(k_i) = \\ &= \prod_{i=1}^n \frac{I(k_i)}{\tilde{I}(k_i)} \prod_{j=1}^n \left(\frac{1}{p_1 \cdot k_j} + \frac{1}{p_2 \cdot k_j} + \frac{1}{p_3 \cdot k_j} + \frac{1}{p_4 \cdot k_j} \right) \end{aligned} \quad (\text{A.5})$$

We have to sample the second product in the right hand side of the above relation, which can be expanded as a sum of terms. The sum is done via Monte Carlo by choosing randomly for each of the photons a fermion to generate its angle according to $1/p \cdot k$. If n_i is the number of photons ‘‘attached’’ to the fermion i , a single term of the sum takes the form

$$\prod_{i=1}^{n_1} \frac{1}{p_1 \cdot k_i} \prod_{j=1}^{n_2} \frac{1}{p_2 \cdot k_j} \prod_{l=1}^{n_3} \frac{1}{p_3 \cdot k_l} \prod_{m=1}^{n_4} \frac{1}{p_4 \cdot k_m} \quad (\text{A.6})$$

The sampling of the angular structure of the previous formula is not trivial. The initial-state sampling (i.e. $1/p_{1,2} \cdot k$) is easy, being the momenta $p_{1,2}$ fixed, while to sample final-state singularities the following problem arises: considering for example the case $n = 2$ with $n_3 = 1$ and $n_4 = 1$ and that we choose the angles of p_3 as independent variables for the phase space integral, Eq. (A.6) says we have to generate the k_1 angles along the p_3 direction according to $\propto 1/p_3 \cdot k_1$ and the k_2 angles along p_4 . The point is that the direction of p_4 can not be defined until all the other momenta are generated. We by-pass the problem by using a multi-channel approach. In the case we are considering, we write

$$\begin{aligned} \frac{1}{p_3 \cdot k_1} \frac{1}{p_4 \cdot k_2} &= \frac{1}{p_3 \cdot k_1} \frac{1}{p_4 \cdot k_2} \frac{\frac{1}{p_3 \cdot k_1}}{\frac{1}{p_3 \cdot k_1} + \frac{1}{p_4 \cdot k_2}} + \\ &+ \frac{1}{p_3 \cdot k_1} \frac{1}{p_4 \cdot k_2} \frac{\frac{1}{p_4 \cdot k_2}}{\frac{1}{p_3 \cdot k_1} + \frac{1}{p_4 \cdot k_2}} \end{aligned} \quad (\text{A.7})$$

The above sum is done again by Monte Carlo, integrating the phase space by using as independent variables the angles of the final-state electron (p_3) in the first term of the sum and the angles of the final-state positron (p_4) in the

second one. In the first term we generate k_1 along p_3 and k_2 along a direction which is not exactly that of p_4 , being the $1/p_4 \cdot k_2$ peak flattened in any case by the denominator $1/p_3 \cdot k_1 + 1/p_4 \cdot k_2$. In the second term the role of p_3 and p_4 are exchanged.

The generalization of Eq. (A.7) to the case n_3 and $n_4 \neq 1$ reads

$$\begin{aligned} \prod_{i=1}^{n_3} \frac{1}{p_3 \cdot k_i} \prod_{j=1}^{n_4} \frac{1}{p_4 \cdot k_j} &= \prod_{i=1}^{n_3} \frac{1}{p_3 \cdot k_i} \prod_{j=1}^{n_4} \frac{1}{p_4 \cdot k_j} \frac{\prod_{i=1}^{n_3} \frac{1}{p_3 \cdot k_i}}{\prod_{i=1}^{n_3} \frac{1}{p_3 \cdot k_i} + \prod_{j=1}^{n_4} \frac{1}{p_4 \cdot k_j}} + \\ &+ \prod_{i=1}^{n_3} \frac{1}{p_3 \cdot k_i} \prod_{j=1}^{n_4} \frac{1}{p_4 \cdot k_j} \frac{\prod_{j=1}^{n_4} \frac{1}{p_4 \cdot k_j}}{\prod_{i=1}^{n_3} \frac{1}{p_3 \cdot k_i} + \prod_{j=1}^{n_4} \frac{1}{p_4 \cdot k_j}} \end{aligned} \quad (\text{A.8})$$

which suggests a similar generation of the independent variables.

References

- [1] Proceedings of the Workshop on Hadronic Cross-Section at Low-Energy (SIGHAD03), Pisa, Italy, 8-10 Oct 2003, Nucl. Phys. **B 131** (Proc. Suppl.) (2004)
- [2] M. Passera, Nucl. Phys. **B 155** (Proc. Suppl.) (2006) 365 [arXiv:hep-ph/0509372]
- [3] F. Jegerlehner, in [1], 213 [arXiv:hep-ph/0312372];
S. Eidelman and F. Jegerlehner, Z. Phys. **C 67** (1995) 585 [arXiv:hep-ph/9502298]
- [4] B. Pietrzyk, in [1], 97
- [5] Z. Zhao, in [1], 223
- [6] S.I. Eidelman (for CMD-2 and SND collaborations), Nucl. Phys. **B 144** (Proc. Suppl.) (2005) 223
- [7] G. Rong (for the BES collaboration), AIP Conf. Proc. **814** (2006) 414
- [8] D. Besson et al. (CLEO collaboration), Phys. Rev. Lett. **96** (2006) 092002 [arXiv:hep-ex/0512038]
- [9] H. Czyż, “The Radiative return method: A Short theory review”, to appear in the proceedings of the conference “ e^+e^- Collisions from ϕ to ψ ”, Novosibirsk (Russia), 27 February - 2 March 2006 [arXiv:hep-ph/0606227];
H. Czyż et al., Eur. Phys. J. **C 39** (2005) 411 [arXiv:hep-ph/0404078];
H. Czyż et al., Eur. Phys. J. **C 27** (2003) 563 [arXiv:hep-ph/0212225];
G. Rodrigo et al., Eur. Phys. J. **C 24** (2002) 71 [arXiv:hep-ph/0112184];
F. Binner et al., Phys. Lett. **B 459** (1999) 279 [arXiv:hep-ph/9902399]

- [10] A. Aloisio et al. (KLOE collaboration), Phys. Lett. **B 606** (2005) 12 [arXiv:hep-ex/0407048]
- [11] B. Aubert et al. (BABAR collaboration), Phys. Rev. **D 73** (2006) 052003 [arXiv:hep-ex/0602006];
Phys. Rev. **D 73** (2006) 012005 [arXiv:hep-ex/0512023]
- [12] C.M. Carloni Calame et al., in [1], 48 [arXiv:hep-ph/0312014];
C.M. Carloni Calame et al., Nucl. Phys. **B 584** (2000) 459 [arXiv:hep-ph/0003268]
- [13] C.M. Carloni Calame, Phys. Lett. **B 520** (2001) 16 [arXiv:hep-ph/0103117]
- [14] A.B. Arbuzov et al., “Monte-Carlo generator for e^+e^- annihilation into lepton and hadron pairs with precise radiative corrections” [arXiv:hep-ph/0504233]
- [15] E. Drago and G. Venanzoni, “A Bhabha generator for DAΦNE including radiative corrections and Φ resonance” INFN/AE-97/48, 1997
- [16] F.A. Berends and R. Kleiss, Nucl. Phys. **B 228** (1983) 537
- [17] S. Jadach et al., Phys. Lett. **B 390** (1997) 298 [arXiv:hep-ph/9608412]
- [18] F. Ambrosino et al. (KLOE collaboration), Eur. Phys. J. **C 47** (2006) 589 [arXiv:hep-ex/0604048];
A. Denig and F. Nguyen, “The KLOE luminosity measurement”, KLOE note 202, July 2005
- [19] R. Bonciani and A. Ferroglia, Nucl. Phys. **B 157** (Proc. Suppl.) (2006) 11 [arXiv:hep-ph/0601246]
- [20] A.B. Arbuzov and E.S. Sherbakova, “Next-to-leading order corrections to Bhabha scattering in renormalization group approach (I). Soft and virtual photonic contributions”, [arXiv:hep-ph/0602119]
- [21] A.A. Penin, Nucl. Phys. **B 734** (2006) 185 [arXiv:hep-ph/0508127];
A.A. Penin, Phys. Rev. Lett. **95** (2005) 010408 [arXiv:hep-ph/0501120]
- [22] R. Bonciani et al., Nucl. Phys. **B 716** (2005) 280 [arXiv:hep-ph/0411321];
R. Bonciani et al., Nucl. Phys. **B 701** (2004) 121 [arXiv:hep-ph/0405275];
R. Bonciani et al., Nucl. Phys. **B 690** (2004) 138 [arXiv:hep-ph/0311145];
R. Bonciani et al., Nucl. Phys. **B 681** (2004) 261; Erratum *ibid.* **B 702** (2004) 364 [arXiv:hep-ph/0310333];
R. Bonciani et al., Nucl. Phys. **B 676** (2004) 399 [arXiv:hep-ph/0307295];
R. Bonciani et al., Nucl. Phys. **B 661** (2003) 289; Erratum *ibid.* **B 702** (2004) [arXiv:hep-ph/0301170]
- [23] R. Bonciani and A. Ferroglia, Phys. Rev. **D 72** (2005) 056004 [arXiv:hep-ph/0507047]
- [24] M. Czakon et al., “The Planar four-point master integrals for massive two-loop Bhabha scattering” [arXiv:hep-ph/0604101];
M. Czakon et al., Phys. Rev. **D 71** (2005) 073009 [arXiv:hep-ph/0412164];

- M. Czakon et al., Nucl. Phys. **B 135** (Proc. Suppl.) (2004) 83 [arXiv:hep-ph/0406203]
- [25] M.N. Achasov et al., “Update of the $e^+e^- \rightarrow \pi^+ + \pi^-$ cross section measured by SND detector in the energy region $400 < \sqrt{s} < 1000$ MeV” [arXiv:hep-ex/0605013]
- [26] D.R. Yennie, S.C. Frautschi and H. Suura, Annals of Physics **13** (1961) 379; S. Jadach and B.F.L. Ward, in proceedings of the “Workshop on Radiative Corrections”, p. 325, Brighton, England, July 9-14, 1989
- [27] <http://www.pv.infn.it/hepcomplex/babayaga.html>
- [28] J.A.M. Vermaseren, “New features of FORM” [arXiv:math-ph/0010025]
- [29] F. Caravaglios and M. Moretti, Phys. Lett. **B 358** (1995), 332 [arXiv:hep-ph/9507237]
- [30] M. Caffo et al., in *Z Physics at LEP1*, G. Altarelli, R. Kleiss and C. Verzegnassi eds., CERN Report **89-08** (CERN, Geneva, 1989), Vol. 1, 171; M. Greco, Riv. Nuovo Cim. **11** (1988) 1
- [31] H. Burkhardt et al., Z. Phys. **C 43** (1989) 497; F. Jegerlehner, Z. Phys. **C 32** (1986) 195
- [32] G. Montagna et al., Phys. Lett. **B 385** (1996) 348 [arXiv:hep-ph/9605252]
- [33] derived from M. Cacciari et al., Comput. Phys. Comm. **90** (1995) 301 [arXiv:hep-ph/9507245]
- [34] S. Jadach et al., Phys. Rev. **D 55** (1997) 3; B.A. Kniehl, Phys. Lett. **B 237**, (1990) 127; G.J.H. Burgers, Phys. Lett **B 164**, (1985) 167; R. Barbieri et al., Nuovo Cim. **A 11** (1972) 824
- [35] A.B. Arbuzov et al., Phys. Atom. Nucl. **60** (1997) 591
- [36] A.B. Arbuzov et al., Nucl. Phys. **B 485** (1997) 457 [arXiv:hep-ph/9512344]
- [37] G. Montagna et al., Nucl. Phys. **B 547** (1999) 39 [arXiv:hep-ph/9811436]
- [38] S. Jadach et al., Phys. Lett. **B 450** (1999) 262 [arXiv:hep-ph/9811245]; S. Jadach et al., Phys. Lett. **B 377** (1996) 168 [arXiv:hep-ph/9603248]
- [39] S. Jadach et al., Phys. Rev. **D 65** (2002) 073030 [arXiv:hep-ph/0109279]; H. Czyz et al., Eur. Phys. J. **C 33** (2004) 333 [arXiv:hep-ph/0308312]
- [40] S. Jadach, O. Nicrosini et al., “Event generators for Bhabha scattering”, in “Physics at LEP2”, CERN-96-01, Vol. 2, pg. 229, G. Altarelli, T. Sjöstrand and F. Zwirner eds. [arXiv:hep-ph/9602393]
- [41] See, for example, Z. Nagy and D.E. Soper, “QCD and Monte Carlo generators” [arXiv:hep-ph/0607046], and references therein
- [42] S. Jadach et al., Phys. Lett. **B 377** (1996) 168 [arXiv:hep-ph/9603248]; A.B. Arbuzov et al., Phys. Lett. **B 383** (1996) 238 [arXiv:hep-ph/9605239]